Enclosure
Relief Request 52 Proposed Alternative in Accordance with
10 CFR 50.55a(a)(3)(i)

ATTACHMENT 3

Weld Residual Stress Analysis for PVNGS Unit 3 RV BMI Nozzle Repair

CALCULATION SUMMARY SHEET (CSS)

AREVA

Document No. ___32___ - ___9219662___ - ___000___   Safety Related: ☒Yes ☐ No

Title ___Weld Residual Stress Analysis for PVNGS3 RV BMI Nozzle Repair (Non-Proprietary)___

PURPOSE AND SUMMARY OF RESULTS:

AREVA Inc. proprietary information in the document is indicated by pairs of braces "[ ]".

PURPOSE:

Visual inspection of the reactor vessel Bottom Mounted Instrument (BMI) nozzles at Palo Verde Nuclear Generation Station, Unit 3 (PVNGS3), in October of 2013 revealed the presence of boric acid crystals on the outside of the lower head at BMI nozzle #3. Boric acid deposits at the gap between the nozzle and head indicate leakage of primary water through cracks in the J-Groove weld and the nozzle wall. AREVA performed a half nozzle repair of nozzle #3 that maintained the full incore instrumentation functionality of the nozzle. This repair, described in References [1] and [2], moves the primary pressure boundary nozzle weld from the inside of the vessel to a weld pad on the outside surface.

The purpose of this report is to document the weld residual stress (WRS) finite element analysis of the as-left J-Groove weld for use in subsequent fracture mechanics analysis.

SUMMARY OF RESULTS:

A WRS analysis of the as-left J-Groove weld on reactor vessel BMI nozzle #3 at Palo Verde Unit 3 has been performed. Appendix B and Appendix C provide stress results for use in downstream fracture mechanics analyses.

This is the Non-Proprietary version of 32-9215089-001.

The following table summarizes the total pages contained in this document.

Section	Main Body	Appendix A	Appendix B	Appendix C	Total
Pages	23	3	3	12	41

THE FOLLOWING COMPUTER CODES HAVE BEEN USED IN THIS DOCUMENT:

CODE/VERSION/REV   CODE/VERSION/REV

___ANSYS 14.5.7 / Windows 7___   _____

THE DOCUMENT CONTAINS ASSUMPTIONS THAT SHALL BE VERIFIED PRIOR TO USE

☐Yes

☒ No

Weld Residual Stress Analysis for PVNGS3 RV BMI Nozzle Repair (Non-Proprietary)

Review Method: ☒ Design Review (Detailed Check)

☐ Alternate Calculation

Signature Block

Name and Title (printed or typed)	Signature	P/R/A and LP/LR	Date	Pages/Sections Prepared/Reviewed/Approved
Tom Riordan Engineer III		P	18APR2014	All
Silvester Noronha Principal Engineer		R	4|18|14	All
Tim Wiger Engineering Manager		A	4/18/14	All

Note: P/R/A designates Preparer (P), Reviewer (R), Approver (A);
LP/LR designates Lead Preparer (LP), Lead Reviewer (LR)

Project Manager Approval of Customer References (N/A if not applicable)

Name (printed or typed)	Title (printed or typed)	Signature	Date
Maya Chandrashekhar	Project Manager		04/18/14

Mentoring Information (not required per 0402-01)

Name (printed or typed)	Title (printed or typed)	Mentor to: (P/R)	Signature	Date
N/A				

Record of Revision

Revision No.	Pages/Sections/Paragraphs Changed	Brief Description / Change Authorization
000	All	Original Release

Weld Residual Stress Analysis for PVNGS3 RV BMI Nozzle Repair (Non-Proprietary)

Table of Contents

List of Tables

List of Figures

1.0   PURPOSE

Visual inspection of the reactor vessel Bottom Mounted Instrument (BMI) nozzles at Palo Verde Nuclear Generation Station, Unit 3 (PVNGS3), in October of 2013 revealed the presence of boric acid crystals on the outside of the lower head at BMI nozzle #3. Boric acid deposits at the gap between the nozzle and head indicate leakage of primary water through cracks in the J-Groove weld and the nozzle wall. AREVA performed a half nozzle repair of nozzle #3 that maintained the full incore instrumentation functionality of the nozzle. This repair, described in References [1] and [2], moves the primary pressure boundary nozzle weld from the inside of the vessel to a weld pad on the outside surface. AREVA Document 51-9220420 (latest revision) provides a road map of the AREVA analyses for the Palo Verde BMI Nozzle.

The purpose of this report is to document the weld residual stress (WRS) finite element analysis of the as-left J-Groove weld for use in subsequent fracture mechanics analysis.

2.0   ANALYTICAL METHODOLOGY

The WRS finite element analysis is carried out utilizing the methodology developed in Reference [3]. The methodology developed in Reference [3] has been successfully benchmarked to mock-up samples and industry round-robin tests in papers such as References [4] and [5], which gives a high level of confidence in its predictive capabilities. In addition, the methodology is consistent with the general recommendations of industry WRS modeling guidance documents such as MRP-317 (Reference [6]).

The fabrication history of BMI nozzle #3 is simulated by the three-dimensional finite element model using the following sequential steps:

1. Multi-pass welding of the Alloy 182 J-Groove buttering. A total of five analytical weld beads are utilized for the buttering weld.

2. Post-weld heat treatment (PWHT) of the buttered low alloy steel head. Note that the stainless steel cladding has already been added to the inner surface of the head as stress free material.

3. Multi-pass J-Groove welding of the original Alloy 600 nozzle to the buttered low alloy steel head. A total of 15 analytical weld beads are used for the J-Groove weld.

4. Hypothetical weld repair by removal of a portion of the J-Groove weld and re-welding this area. A total 10 analytical weld beads covering half the circumference were removed and re-welded for the J-Groove weld repair.

5. Hydrostatic pressure testing performed in the shop and field.

6. Three cycles of operating conditions at steady state pressure and temperature. These multiple static load steps are meant to capture any "shakedown" of residual stress with operation.

7. Removal of the boat sample and severing the existing nozzle at the appropriate elevation.

The general purpose finite element code ANSYS is used to perform the WRS finite element analysis. The finite element analysis is based on a 3-dimensional model. The basic steps comprising the multi-pass welding simulation of the buttering, and J-Groove weld are as follows:

```



```

Static load steps are applied to simulate hydrostatic testing and operation after the simulation of the J-Groove welding. Additional static load steps are used to simulate the boat sample removal and severing of the existing nozzle at an appropriate elevation.

3.0 ASSUMPTIONS

3.1 Unverified Assumptions

No unverified assumptions are used in this calculation.

3.2 Justified Assumptions

The following justified assumptions are used in this calculation:

1. Cladding is added to the Reactor Vessel Bottom Head (RVBH) as stress free material. This is a reasonable assumption since the RVBH along with the cladding receives post-weld heat treatment.

2. The recently performed half-nozzle repair weld at the OD surface (Reference [2]) is not modeled; since this area is remote from the as-left J-Groove weld the impact on the stresses in the as-left J-Groove weld will be negligible. Additionally, it is expected that the residual stresses from the repair pad welding would be tensile in the deposited repair weld pad balanced by compressive stresses in the RVBH; thus the simplification is conservative for the as-left weld since no credit would be taken for any compressive stress induced by the repair.

3.3 Modeling Simplifications

The following modeling simplifications are used in this calculation:

1. A half model is considered due to the symmetry of the components.

2. The boat sample geometry (Reference [7]) is approximated, as described in the following sentences. The boat sample removal is simulated by selecting and "killing" a set of elements, which results in a "jagged" boundary. This approach is taken in order to maintain a high quality hexahedral mesh for the rest of the simulation. This approach is reasonable since the impact of the resultant geometry on stresses will be local to the elements near this "jagged" boundary and overall equilibrium is maintained in the finite element solution. Additionally, the boat sample is considered to be centered on the symmetry plane on the uphill side in order to maintain a symmetric model.

3. There is no contribution to the WRS field predicted in this document due to any interaction with the surrounding penetrations. This is a reasonable assumption since the surrounding penetrations are spaced far enough away from the modeled BMI nozzle penetration to preclude interaction of the residual stress fields.

4. Simulation of PWHT does not include creep. This is a conservative simplification since creep would reduce the residual stress in the RVBH and butter.

5. The weld bead sequence follows the recommendation of Reference [8] to the extent practical, however, the analytical weld beads typically lump together several actual weld beads, which is an acceptable practice in numerical welding simulations. The welding simulation performed here uses five analytical weld beads for the buttering weld passes, 15 analytical weld beads for the J–Groove weld passes, and 10 analytical weld beads covering half the circumference for the J-Groove weld repair passes. The analytical weld beads and pass sequence are shown in Figure 4-4, Figure 4-5, and Figure 4-6.

4.0 DESIGN INPUTS

4.1 Geometry

Details of the geometry are provided in References [9], [10], [11], and [12]. Key dimensions are listed in Table 4-1.

Table 4-1: Key Dimensions

Description	Value	Reference/Comments
RVBH Inside Radius	[ ]	Reference [9]
RVBH Thickness	[ ]	Reference [9]
Cladding Thickness	[ ]	Reference [9]
Nozzle OD	[ ]	Reference [10]
Nozzle ID	[ ]	Reference [10]
Height of J-Groove plus Fillet	[ ]	Reference [11]
Butter Thickness	[ ]	Reference [12]

AREVA

4.2　Materials

The materials of each component are listed in Table 4-2.

Table 4-2:　Component Materials

Component	Material	Reference/Comments
RVBH	SA-533 Grade B Class 1	Reference [1]
BMI Nozzle	SB-166 Alloy 600	Reference [1]
Cladding	Austenitic Stainless Steel (304)	Reference [1], 18-24Cr, 8-12Ni per Reference [18], Section 4.7.4
Buttering	Alloy 182 (ENiCrFe-3)	Reference [1]
J-Groove Weld	Alloy 82 (ERNiCr-3)	Reference [1]

The analysis in this calculation uses physical properties (thermal conductivity, specific heat, density, mean coefficient of thermal expansion, elastic modulus, and Poisson's ratio) from Reference [13]. Properties for SA-533, Grade B, Class 1 are not directly available in Reference [13]; properties from SA-508 are utilized since they were found to be similar for both low alloy steels based on review of original construction code (Reference [14]), which provides the same specified minimum yield and tensile strengths for both materials as well as the same thermal and mechanical properties. All physical and mechanical properties except Poisson's ratio are temperature dependent; these properties are defined in ANSYS input file "thermo_mech.inp". The room temperature thermal and mechanical properties used in the analysis are provided in Table 4-3.

Table 4-3:　Room Temperature Thermal and Mechanical Properties

	SA-533	Alloy 600	Alloy 82/182	304 Stainless
Density (lbm/in^3)	[　　]	[　　]	[　　]	[　　]
Thermal Conductivity (BTU/s-in-°F)	[　　]	[　　]	[　　]	[　　]
Specific Heat (BTU/lbm-°F)	[　　]	[　　]	[　　]	[　　]
Elastic Modulus (psi)	[　　]	[　　]	[　　]	[　　]
Poisson's Ratio (-)	[　]	[　]	[　]	[　]
Mean CTE (/°F)	[　　]	[　　]	[　　]	[　　]

The temperature dependent stress-strain curves for each material are also from Reference [13]. Stress-strain curves for the SA-533 and the Alloy 600 have been modified slightly based on the CMTRs (References [15] and [16]) for these materials using the following procedure:

1. Calculate the ratios of room temperature yield and ultimate strength from the CMTRs to the room temperature values from the WRS materials database (Reference [13]). Note that the values from the WRS database are first converted to engineering stress to be consistent with the CMTR data.

2. Multiply the WRS database yield and ultimate stress values at each temperature by these ratios. For points between yield and ultimate a ratio is determined by linear interpolation between the yield ratio and ultimate ratio based on strain.

3. For the SA-533 material the ratio of yield stress was higher than the ratio of ultimate stress. At high temperatures where the stress-strain curves are nearly perfectly plastic steps 1 and 2 can result in yield

Weld Residual Stress Analysis for PVNGS3 RV BMI Nozzle Repair (Non-Proprietary)

stresses higher than ultimate; in these cases all values higher than the calculated ultimate stress were set equal to the calculated ultimate stress.

The above procedure results in the WRS simulation using room temperature stress strain curves for the Alloy 600 and SA-533 that have yield and ultimate strengths approximately equal to those from the CMTRs. This increased the SA-533 stress-strain curves [   ] over the WRS database values (Reference [13]) and decreased the Alloy 600 stress-strain curves [   ] from the WRS database values (Reference [13]). The resulting temperature dependent true stress-strain curves are defined utilizing the multi-linear kinematic hardening model in ANSYS input file "kinh_props-CMTR.inp". The room temperature true stress-true plastic strain curves utilized are shown in Figure 4-1.

Figure 4-1: Room Temperature True Stress-True Plastic Strain Curves

Weld Residual Stress Analysis for PVNGS3 RV BMI Nozzle Repair (Non-Proprietary)

4.3   Welding Parameters

The welding process parameter assumptions provided in Reference [8] are utilized to establish the welding heat generation in the finite element model of the butter, J-Groove weld, and the hypothetical J-Groove weld repair. The parameters utilized are provided in Table 4-4. The analytical weld bead sequences are shown in Figure 4-4, Figure 4-5, and Figure 4-6. Based on the information provided in Reference [8], the hypothetical J-Groove weld repair shown in Figure 4-6 is postulated to cover one half of the circumference and replaces 10 of the original 15 analytical weld beads.

Table 4-4: Welding Parameters

Parameter	Value	Units	Reference/Comments
Butter Layer/s			
Current	[ ]	Amps	Reference [8], average of two layers
Voltage	[ ]	Volts	Reference [8], average of two layers
Travel Speed	[ ]	in/min	Reference [8], average of two layers
Arc Efficiency	[ ]	-	Reference [3]
Maximum Interpass Temperature	[ ]	°F	Reference [3]
J-Groove Layers 1-3*			
Current	[ ]	Amps	Reference [8]
Voltage	[ ]	Volts	Reference [8]
Travel Speed	[ ]	in/min	Reference [8]
Arc Efficiency	[ ]	-	Reference [3]
Maximum Interpass Temperature	[ ]	°F	Reference [3]
J-Groove Balance of Layers and Hypothetical J-Groove Repair**			
Current	[ ]	Amps	Reference [8]
Voltage	[ ]	Volts	Reference [8]
Travel Speed	[ ]	in/min	Reference [8]
Arc Efficiency	[ ]	-	Reference [3]
Maximum Interpass Temperature	[ ]	°F	Reference [3]

*Used for analytical J-Groove weld beads 1-3.
**Used for all other analytical J-Groove weld beads and the hypothetical J-Groove repair weld.

AREVA

4.4 Finite Element Model

The finite element model utilized is a three-dimensional half symmetry model. The mesh consists of 8-node brick elements which are ANSYS element type SOLID70 for thermal analyses and SOLID185 for stress analyses. CONTA174 and TARGE170 elements are used to simulate contact between the nozzle and the RVBH. Weld metal deposition and material removal are simulated using the ANSYS elements "birth and death" feature. The finite element model is documented in the ANSYS input file "BMI_Nozzle_3.inp".

The finite element mesh is shown in Figure 4-2 and Figure 4-3. The weld passes utilized for the butter, J-Groove weld, and J-Groove weld repair are based on the recommendations in Reference [8]; the pass sequences are depicted in Figure 4-4, Figure 4-5, and Figure 4-6.

Figure 4-2: WRS Finite Element Model Isometric View

Weld Residual Stress Analysis for PVNGS3 RV BMI Nozzle Repair (Non-Proprietary)

Figure 4-3: Weld Region Mesh

Figure 4-4: Butter Pass Sequence

Weld Residual Stress Analysis for PVNGS3 RV BMI Nozzle Repair (Non-Proprietary)

Figure 4-5: J-Groove Weld Pass Sequence

Figure 4-6: Hypothetical Repair Weld Pass Sequence

4.5 Boundary Conditions

4.5.1 Thermal Boundary Conditions

The thermal model is loaded by volumetric heat generation in the elements of the weld pass being deposited. An adiabatic boundary condition is applied to the model symmetry plane and the RVBH cutting planes. Heat loss from the inner and outer surfaces is simulated using a heat transfer coefficient of [   ] per the Reference [3] WRS procedure to model natural convection to air. Radiation boundary conditions are not considered since radiation losses from the molten weld pool are included in the weld efficiency.

The thermal simulations for the buttering, J-Groove weld, and the J-Groove weld repair are performed by the input files "Thermal_Butter.inp", "Thermal_JGW.inp", and "Thermal_JGW_Repair.inp", respectively.

4.5.2 Structural Boundary Conditions

The structural simulations consist of buttering, PWHT, J-Groove weld passes, J-Groove weld repair, hydrostatic test, operating cycles and boat sample removal. In all cases, rigid body motion is eliminated by restraining displacements normal to the symmetry plane and RVBH cutting planes.

For the weld pass simulations, temperature histories from the thermal analyses are used as thermal loads in the structural analysis. A traction free boundary condition (i.e., no applied forces) is maintained on all external surfaces of the model. Weld pass simulations for the buttering, J-Groove weld, and the J-Groove weld repair are performed by the input files "Stress_Butter.inp", "Stress_JGW.inp", and "Stress_JGW_Repair.inp", respectively.

PWHT of the RVBH, clad and butter is simulated by applying a uniform temperature of [   ], which is the PWHT temperature for the RVBH material per Reference [17]. A traction free boundary condition is maintained on all external surfaces of the model. The PWHT analysis is performed by the input file "Stress_PWHT.inp".

Following the completion of the weld pass simulations, two hydrostatic test cycles apply a pressure of [   ] on the wetted surfaces and a uniform temperature of [   ] (Reference [18], page 11). Subsequently, three cycles of normal operating conditions are simulated using the normal operating pressure of [   ] on the wetted surfaces and a uniform temperature equal to the inlet water temperature of [   ] (Reference [18], page 10). The condition with a temperature of [   ] with a pressure of [   ] is subsequently referred to as "operating" or "operating condition" in this calculation. The hydrostatic test and operating cycles are simulated using the input file "Stress_HydroOpCond.inp".

The boat sample removal and nozzle severing are simulated by "killing" the relevant elements and solving with no loads applied at a temperature of [   ]. The condition with a temperature of [   ] with no loads applied is subsequently referred to as "cold shutdown" in this calculation. Simulation of the boat sample removal and nozzle severing is performed by the input file "Stress_Boat.inp". Elements "killed" to simulate the boat sample and cutting of the nozzle are indicated in Figure 4-7 and shown as removed in Figure 4-8.

Weld Residual Stress Analysis for PVNGS3 RV BMI Nozzle Repair (Non-Proprietary)

Figure 4-7: Elements to be Removed for Boat Sample Removal and Nozzle Severing Marked

Figure 4-8: Boat Sample Removal and Nozzle Severing

5.0 COMPUTER USAGE

5.1 Software

ANSYS Version 14.5.7 (Reference [19]) was used in this analysis. All modeling and analyses were performed on the following computer:

- DELL Precision M6600, Intel(R) Core(TM) i7-2640M CPU @ 2.80GHz, 8GB of RAM
- Operating System: Windows 7, Service Pack 1, 64 Bit
- Name of person running tests: Tom Riordan
- Date of Tests: January 14, 2014

The test problems vm32mod2d, v32mod3d, vm38mod2d, and vm38mod3d were executed with acceptable results. See Appendix A for details of the test cases.

5.2 Computer Files

The ANSYS input and output files are listed in Table 5-1. Files are store in ColdStor at the following path:

\cold\General-Access\32\32-9000000\32-9215089-000\official

Table 5-1: Computer Files

Size (Bytes)	Date	Time	File Name
./AppC:			
1413	Jan 17 2014	13:03:38	Stress_Op.inp
10252	Jan 17 2014	14:03:33	Stress_Op.out
1779	Jan 21 2014	11:40:21	WRS_OP_mb_sum.dat
1779	Mar 11 2014	6:47:01	WRS_OP_mb_sum_ax.dat
87023	Jan 21 2014	11:40:21	WRS_OP_paths.dat
87023	Mar 11 2014	6:47:01	WRS_OP_paths_ax.dat
1779	Jan 21 2014	11:40:39	WRS_mb_sum.dat
1779	Mar 11 2014	6:47:21	WRS_mb_sum_ax.dat
87023	Jan 21 2014	11:40:39	WRS_paths.dat
87023	Mar 11 2014	6:47:21	WRS_paths_ax.dat
1959	Jan 21 2014	9:54:47	linearize.mac
1965	Mar 11 2014	6:41:59	linearize_ax.mac
261	Jan 21 2014	9:23:08	loc_data.inp
3476	Jan 21 2014	11:35:16	path_results_WRS.inp
35695	Jan 21 2014	11:40:39	path_results_WRS.out
3462	Jan 21 2014	11:26:52	path_results_WRS_OP.inp
35762	Jan 21 2014	11:40:21	path_results_WRS_OP.out
3479	Mar 11 2014	6:46:28	path_results_WRS_OP_ax.inp
35823	Mar 11 2014	6:47:02	path_results_WRS_OP_ax.out
3490	Mar 11 2014	6:46:31	path_results_WRS_ax.inp
35781	Mar 11 2014	6:47:21	path_results_WRS_ax.out

Weld Residual Stress Analysis for PVNGS3 RV BMI Nozzle Repair (Non-Proprietary)

Size (Bytes)	Date	Time	File Name
./Materials:			
4859	Jan 10 2014	13:55:15	kinh_props-CMTR.inp
4494	Dec 10 2013	9:58:46	kinh_props.inp
26432	Dec 03 2013	14:32:01	thermo_mech.inp
./Model:			
11647432	Jan 03 2014	11:27:31	BMI_Nozzle_3.inp
./Post:			
534467	Jan 20 2014	8:08:55	WRS.sav
2061	Jan 15 2014	14:30:00	extract_nodal_stress.inp
18148	Jan 20 2014	8:08:55	extract_nodal_stress.out
./Stress:			
2188	Nov 19 2013	10:46:09	AnnealMaterial3D.mac
855	Jan 17 2014	12:03:41	Stress_Boat.inp
9548	Jan 17 2014	13:12:17	Stress_Boat.out
4683	Jan 10 2014	17:54:28	Stress_Butter.inp
24564	Jan 11 2014	0:12:24	Stress_Butter.out
2268	Jan 03 2014	13:00:42	Stress_HydroOpCond.inp
11477	Jan 12 2014	18:23:02	Stress_HydroOpCond.out
2955	Jan 03 2014	12:24:48	Stress_JGW.inp
20473	Jan 11 2014	22:30:43	Stress_JGW.out
2718	Jan 03 2014	12:28:26	Stress_JGW_Repair.inp
20178	Jan 12 2014	17:42:06	Stress_JGW_Repair.out
899	Dec 02 2013	9:16:26	Stress_PWHT.inp
9474	Jan 11 2014	0:20:30	Stress_PWHT.out
./Thermal:			
576	Feb 16 2012	13:35:22	GetEstTime3.mac
493	Feb 16 2012	13:35:22	Get_DeltaT_Controls.mac
998	Feb 16 2012	13:34:59	Summarize_Weld_Bead_Temp.mac
598	Feb 17 2012	17:03:34	TempCheckCooldown.mac
659	Feb 17 2012	16:55:29	TempCheckHeatup.mac
9901	Dec 16 2013	8:10:07	Thermal_Butter.inp
133351	Jan 08 2014	18:07:55	Thermal_Butter.out
9745	Dec 16 2013	8:12:28	Thermal_JGW.inp
23277	Jan 08 2014	20:09:03	Thermal_JGW.out
8957	Dec 16 2013	8:11:27	Thermal_JGW_Repair.inp
22302	Jan 08 2014	22:29:02	Thermal_JGW_Repair.out

Size (Bytes)	Date	Time	File Name
./Verification:			
3551	Jan 05 2009	9:09:26	vm32mod2D.inp
55666	Jan 14 2014	10:53:11	vm32mod2D.out
624	Jan 14 2014	10:53:11	vm32mod2D.vrt
4940	Jan 06 2009	12:15:42	vm32mod3D.inp
111280	Jan 14 2014	10:53:14	vm32mod3D.out
624	Jan 14 2014	10:53:14	vm32mod3D.vrt
2458	Jan 07 2009	10:28:06	vm38mod2D.inp
14361	Jan 14 2014	10:53:17	vm38mod2D.out
650	Jan 14 2014	10:53:17	vm38mod2D.vrt
3112	Jan 07 2009	10:35:54	vm38mod3D.inp
16834	Jan 14 2014	10:53:20	vm38mod3D.out
650	Jan 14 2014	10:53:19	vm38mod3D.vrt

6.0 CALCULATIONS AND RESULTS

After completion of the J-Groove welding simulation, two hydrostatic test cycles, three normal operating cycles and the removal of the boat sample are simulated. The residual hoop stresses at cold shutdown are shown in Figure 6-1. The residual axial stresses are shown in Figure 6-2.

The subsequent fracture mechanics analysis will utilize explicit crack finite element models for calculation of stress intensity factors for postulated flaws in the J-Groove weld and butter. To facilitate this analysis, nodal hoop stresses on the symmetry plane are extracted and provided in Appendix B.

Appendix C provides results of the case with operating temperature and pressure applied after the removal of the boat sample; stress results on path lines in the nozzle are provided for evaluation of flaws in the nozzle.

AREVA

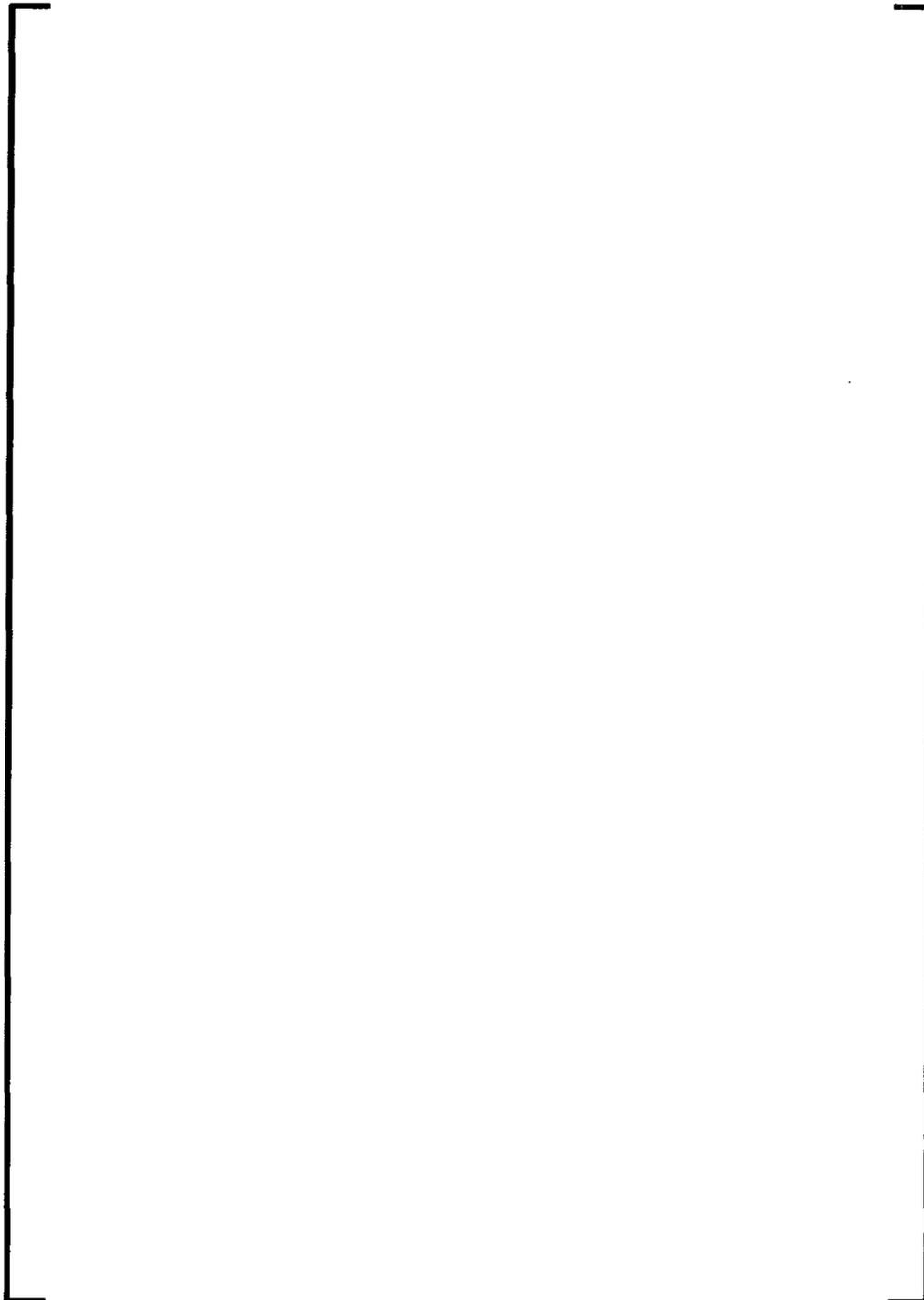Weld Residual Stress Analysis for PVNGS3 RV BMI Nozzle Repair (Non-Proprietary)

Figure 6-1: Residual Hoop Stress (psi) at Cold Shutdown

AREVA
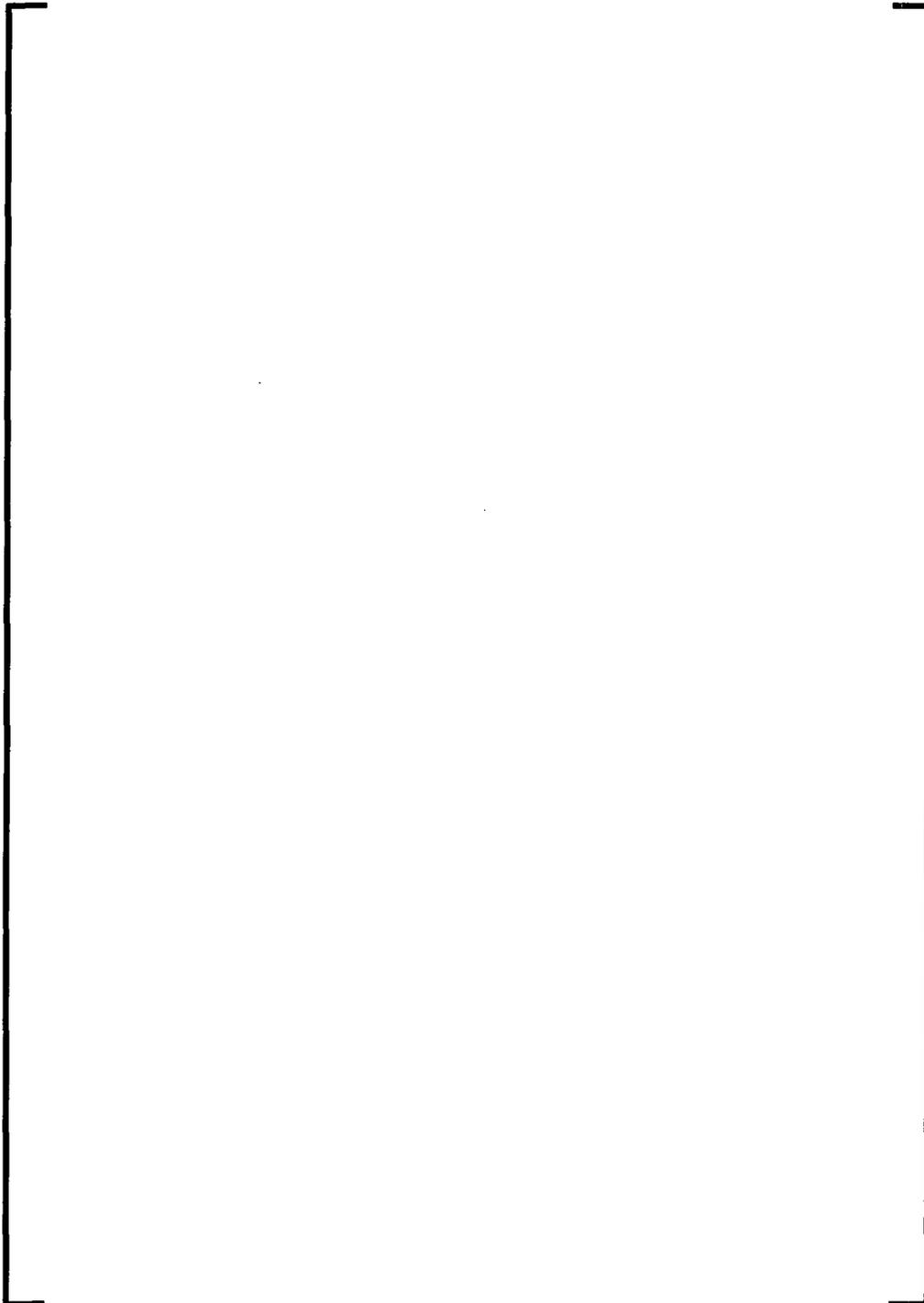
Figure 6-2: Residual Axial Stress (psi) at Cold Shutdown

7.0 REFERENCES

References identified with an (*) are maintained within Palo Verde Nuclear Generating Station Records System and are not retrievable from AREVA Records Management. These are acceptable references per AREVA Administrative Procedure 0402-01, Attachment 8. See page 2 for Project Manager Approval of customer references.

1. AREVA Document 08-9212780-001, "Palo Verde Unit 3 Reactor Vessel Bottom Mounted Instrument Nozzle Modification".
2. AREVA Document 02-9212754E-001, "Palo Verde Unit 3 Bottom Mounted Instrument Nozzle Repair (Penetration 3)".
3. AREVA Document 32-2500013-001, "Technical Basis for Numerical Simulation of Welding Residual Stresses".
4. D.E. Killian, "Design of a Weld Overlay for a Large Bore Pipe Nozzle to Optimize Residual Stress", PVP2010-26100, Proceedings of the ASME 2010 Pressure Vessels & Piping Division Conference, July 18-22, Bellevue, Washington, USA.
5. D.E. Killian, "Validation of Welding Residual Stress Model Using Results from a Pressurizer Surge Nozzle Mockup", PVP2011-57767, Proceedings of the ASME 2011 Pressure Vessels & Piping Division Conference, July 17-21, Baltimore, Maryland, USA.
6. "Materials Reliability Program: Welding Residual Stress Dissimilar Metal Butt-Weld Finite Element Modeling Handbook (MRP-317)". EPRI, Palo Alto, CA: 2011. 1022862.
7. *PVNGS Document N001-0301-00633, Revision 0, "Boat Sample Extraction General Layout Drawing".
8. AREVA Document 51-9213228-001, "Palo Verde Unit 3 – Partial Penetration J-Groove Welding Heat Input Assumptions for Bottom Mounted Instrumentation Nozzle to Head Welding".
9. *PVNGS Document N001-0301-00054, Revision 2, "General Arrangement Arizona Public Service III 182.25 ID Reactor Vessel"
10. *PVNGS Document N001-0603-00208, Revision 3, "Bottom Head Instrument Tubes".
11. *PVNGS Document N001-0301-00527, Revision 0, "Lower Vessel Final Assembly – Arizona Public Service III, 182.25 ID PWR".
12. *PVNGS Document N001-0301-00530, Revision 0, "Bottom Head Penetrations – Arizona Public Service III, 182.25 ID PWR".
13. AREVA Document 32-2500012-002, "Materials Database for Weld Residual Stress Finite Element Analyses".
14. ASME Boiler and Pressure Vessel Code, Section III, "Nuclear Power Plant Components", Division 1, 1971 Edition including Addenda through Winter 1973.
15. *Palo Verde Unit 3 Bottom Head CMTR.
16. *Palo Verde Unit 3 Alloy 600 Bottom Mounted Nozzle CMTR.
17. *PVNGS Document CVER-13-281, "Transmittal of Palo Verde Unit 3 Bottom Head Postweld Heat Treatment (PWHT) and Materials", October 28, 2013.
18. *PVNGS Document N001-0301-00006, Revision 6, "General Specification for Reactor Vessel Assembly".
19. ANSYS Finite Element Computer Code, Version 14.5, ANSYS Inc., Canonsburg, PA.

APPENDIX A: VERIFICATION OF ANSYS COMPUTER CODE

Four verification problems were selected to test key features of the ANSYS finite element computer program (Reference [19]) used in the current numerical welding simulations, the development of thermal stress in a cylinder and the elastic-plastic response of a cylinder under pressure loading.

All test cases executed properly, as demonstrated on the following pages.

Verification Problem VM32MOD
Thermal Stresses in a Long Cylinder

Two-Dimensional Analysis   **File: vm32mod2d.vrt**

```
--------------- VM32MOD2D RESULTS COMPARISON ----------------

                |  TARGET   |   ANSYS   |   RATIO

PLANE55 THERMAL ANALYSIS:

T (C) X=.1875 in     -1.00000     -1.00000    1.000
T (C) X=.2788 in     -0.67037     -0.67039    1.000
T (C) X=0.625 in      0.00000      0.00000    0.000

PLANE182 STATIC ANALYSIS:

A_STS psi X=.187      420.42       429.99     1.023
T_STS psi X=.187      420.42       429.61     1.022
A_STS psi X=.625     -194.58      -205.15     1.054
T_STS psi X=.625     -194.58      -205.08     1.054
```

Three-Dimensional Analysis   **File: vm32mod3d.vrt**

```
--------------- VM32MOD3D RESULTS COMPARISON ----------------

                |  TARGET   |   ANSYS   |   RATIO

SOLID70 THERMAL ANALYSIS:

T (C) X=.1875 in     -1.00000     -1.00000    1.000
T (C) X=.2788 in     -0.67037     -0.67039    1.000
T (C) X=0.625 in      0.00000      0.00000    0.000

SOLID185 STATIC ANALYSIS:

A_STS psi X=.187      420.42       429.67     1.022
T_STS psi X=.187      420.42       430.04     1.023
A_STS psi X=.625     -194.58      -205.11     1.054
T_STS psi X=.625     -194.58      -205.17     1.054
```

Verification Problem VM38MOD

Plastic Loading of a Thick-Walled Cylinder

Two-Dimensional Analysis   **File: vm38mod2d.vrt**

```
---------------- VM38MOD2D RESULTS COMPARISON ----------------

                    |   TARGET   |   ANSYS   |   RATIO

PLANE182 FULLY ELASTIC ANALYSIS (psi):

SIGR    LEFT END        -9984.      -10103.    1.012
SIGT    LEFT END        18645.       18763.    1.006
SIGR    RIGHT END        -468.        -481.    1.028
SIGT    RIGHT END        9128.        9141.    1.001

PLANE182 FULLY PLASTIC ANALYSIS (psi):

SIGEFF  LEFT END        30000.       30000.    1.000
SIGEFF  RIGHT END       30000.       30000.    1.000
Pult                    24011.       23350.    0.972


------------------------------------------------------------
```

Three-Dimensional Analysis   **File: vm38mod3d.vrt**

```
---------------- VM38MOD3D RESULTS COMPARISON ----------------

                    |   TARGET   |   ANSYS   |   RATIO

SOLID185 FULLY ELASTIC ANALYSIS (psi):

SIGR    LEFT END        -9984.      -10066.    1.008
SIGT    LEFT END        18645.       18776.    1.007
SIGR    RIGHT END        -468.        -475.    1.014
SIGT    RIGHT END        9128.        9128.    1.000

SOLID185 FULLY PLASTIC ANALYSIS (psi):

SIGEFF  LEFT END        30000.       30000.    1.000
SIGEFF  RIGHT END       30000.       30000.    1.000
Pult                    24011.       23360.    0.973


------------------------------------------------------------
```

APPENDIX B: WRS RESULTS FOR AS-LEFT J-GROOVE WELD ANALYSIS

This appendix provides the weld residual stress results to be used for evaluation of postulated flaws in the J-Groove weld, butter, head. Node locations on the symmetry plane and the corresponding hoop stresses are extracted and saved in the file "WRS.sav" (see Table 5-1) as ANSYS array parameters. The stresses extracted are from the final step of the WRS simulation, i.e., boat sample removed at cold shutdown. [

]; this ensures that stresses can be mapped to and from the correct body (nozzle or RVBH) in areas where the gap between the two is small. The extraction of the nodal stresses is performed by the file "extract_nodal_stress.inp".

ANSYS arrays containing the extracted data are:

loc_noz = Nozzle node locations (1027×3)
sz_noz = Nozzle hoop stresses (1027×1)
loc = Node locations excluding nozzle (1439×3)
sz = Hoop stresses excluding nozzle (1439×1)

Plots of the extracted hoop stress data are shown in Figure B-1 and Figure B-2.

Weld Residual Stress Analysis for PVNGS3 RV BMI Nozzle Repair (Non-Proprietary)

Figure B-1: Hoop Stresses Excluding Nozzle (psi)

Figure B-2: Nozzle Hoop Stresses (psi)

Weld Residual Stress Analysis for PVNGS3 RV BMI Nozzle Repair (Non-Proprietary)

APPENDIX C: WRS RESULTS FOR NOZZLE FLAW EVALUATION

The purpose of this appendix is to provide WRS results for evaluation of flaws in the existing (remnant) nozzle. Since the remnant nozzle material is Alloy 600 this appendix runs an additional load step in which operating pressure and temperature are applied to the model following removal of the boat sample and the bottom portion of the nozzle; this provides a WRS plus operating stress state for PWSCC flaw growth evaluations. This step is performed by the ANSYS input file "Stress_Op.inp". Contour plots showing the WRS plus operating hoop and axial stress results are shown in Figure C-6 and Figure C-7, respectively.

Stress results will be provided for WRS only at cold shutdown (generated by input files: "path_results_WRS.inp" and "path_results_WRS_ax.inp") as well as the WRS plus operating conditions case (generated by input files: "path_results_WRS_OP.inp" and "path_results_WRS_OP_ax.inp"). [

]

Figure C-1: Paths for Stress Results

Weld Residual Stress Analysis for PVNGS3 RV BMI Nozzle Repair (Non-Proprietary)

Hoop stress results along the path lines are provided in the files below (see also Table 5-1):

"WRS_paths.dat"	=	Path hoop stress results for WRS at cold shutdown.
"WRS_OP_paths.dat"	=	Path hoop stress results for WRS plus Operating Condition.
"WRS_mb_sum.dat"	=	Path hoop membrane and membrane plus bending results for WRS at cold shutdown.
"WRS_OP_mb_sum.dat"	=	Path hoop membrane and membrane plus bending results for WRS plus Operating Condition.
"WRS_paths_ax.dat"	=	Path axial stress results for WRS at cold shutdown.
"WRS_OP_paths_ax.dat"	=	Path axial stress results for WRS plus Operating Condition.
"WRS_mb_sum_ax.dat"	=	Path axial membrane and membrane plus bending results for WRS at cold shutdown.
"WRS_OP_mb_sum_ax.dat"	=	Path axial membrane and membrane plus bending results for WRS plus Operating Condition.

Detailed results of hoop stress vs path location are provided in the "*_paths.dat" and "*_paths_ax.dat" files for each path. [

]

The "*_mb_sum.dat" and "*_mb_sum_ax.dat" files contain membrane and membrane plus bending hoop stress results which are calculated by the ANSYS macro file "linearize.mac" and "linearize_ax.mac". The membrane stress is calculated using numerical integration as follows:

$$\sigma_M = \frac{1}{t}\int_{-t/2}^{t/2}\sigma dx = \frac{1}{x_n - x_1}\sum_{i=1}^{i=n-1}\frac{\sigma_i + \sigma_{i+1}}{2}\Delta x$$

where t is the wall thickness, x is the path coordinate, σ is the stress (hoop or axial), n is the number of points on the path, and Δx is the distance between adjacent points on the path. The bending component of stress is calculated similarly using

$$\sigma_B = \frac{6}{t^2}\int_{-t/2}^{t/2}\sigma(x - x_c)dx = \frac{6}{(x_n - x_1)^2}\sum_{i=1}^{i=n-1}\frac{\sigma_i + \sigma_{i+1}}{2}\left(\frac{x_i + x_{i+1}}{2} - \frac{x_1 + x_n}{2}\right)\Delta x$$

where x_c is the path coordinate of the wall midpoint.

The membrane and membrane plus bending hoop stress results for WRS at cold shutdown (from "WRS_mb_sum.dat") and for WRS plus operating condition (from "WRS_OP_mb_sum.dat") are provided in Table C-1 and Table C-2, respectively. The hoop stresses are plotted in Figure C-2 and Figure C-3. The membrane and membrane plus bending axial stress results for WRS at cold shutdown (from "WRS_mb_sum_ax.dat") and for WRS plus operating condition (from "WRS_OP_mb_sum_ac.dat") are provided in Table C-3 and, Table C-4 respectively. The axial stresses are plotted in Figure C-4 and Figure C-5. Note that cold shutdown and operating condition are as defined in Section 4.5.2. In all cases, the membrane plus bending stress on the OD is membrane stress minus the reported bending stress, and the membrane plus bending on the ID is membrane stress plus the reported bending stress. In all plots the location of path P12 is set to elevation zero and the locations of path P1 and P23 are indicated on each plot. As shown in the tables and plots hoop stresses are dominant.

Weld Residual Stress Analysis for PVNGS3 RV BMI Nozzle Repair (Non-Proprietary)

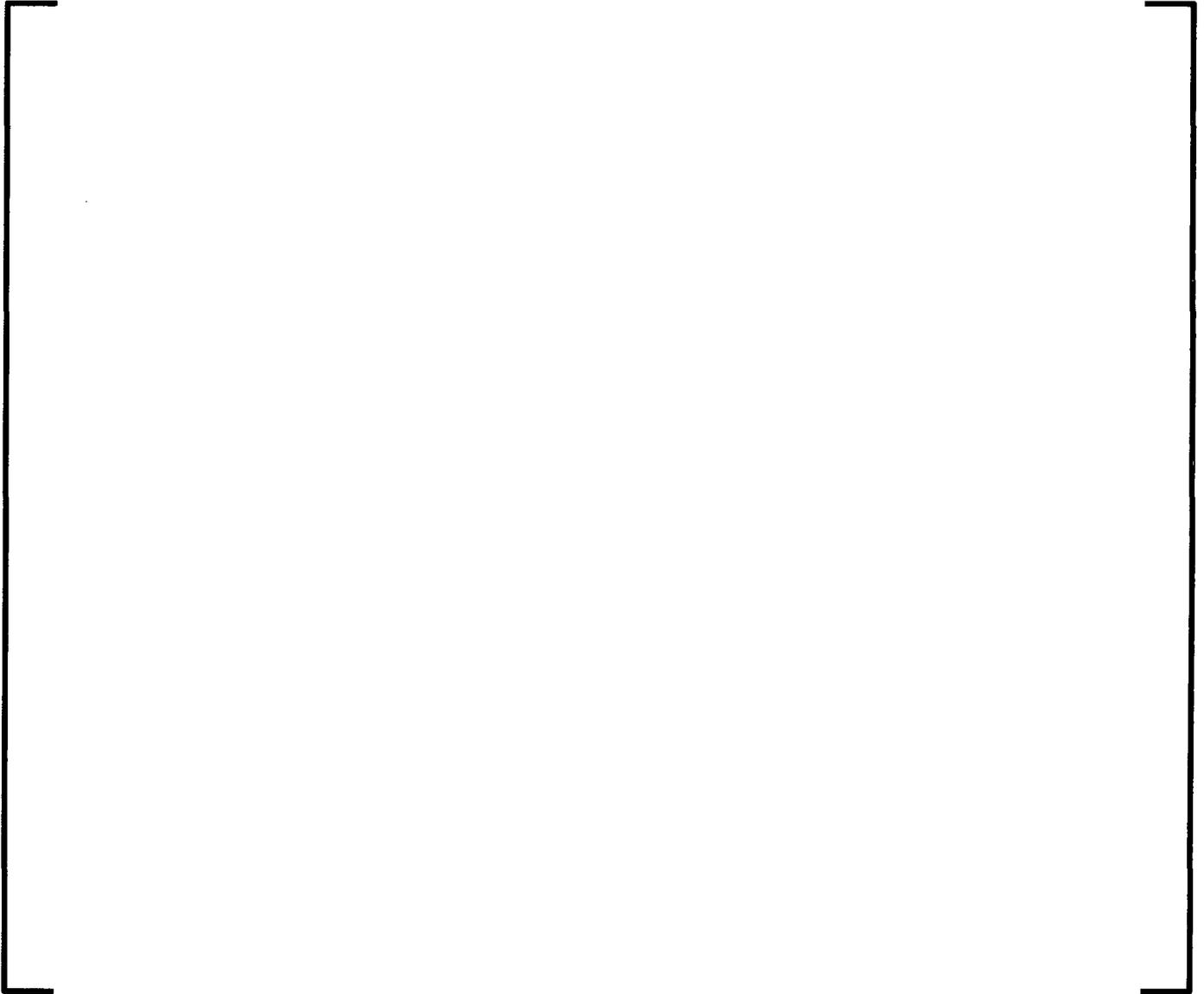**Table C-1: Linearized Hoop Stress Results for WRS at Cold Shutdown**

Weld Residual Stress Analysis for PVNGS3 RV BMI Nozzle Repair (Non-Proprietary)

Figure C-2: Linearized Hoop Stress Results for WRS at Cold Shutdown

Weld Residual Stress Analysis for PVNGS3 RV BMI Nozzle Repair (Non-Proprietary)

Table C-2: Linearized Hoop Stress Results for WRS plus Operating Condition

AREVA

Weld Residual Stress Analysis for PVNGS3 RV BMI Nozzle Repair (Non-Proprietary)

Figure C-3: Linearized Hoop Stress Results for WRS plus Operating Condition

Table C-3: Linearized Axial Stress Results for WRS at Cold Shutdown

Weld Residual Stress Analysis for PVNGS3 RV BMI Nozzle Repair (Non-Proprietary)

Figure C-4: Linearized Axial Stress Results for WRS at Cold Shutdown

Weld Residual Stress Analysis for PVNGS3 RV BMI Nozzle Repair (Non-Proprietary)

Table C-4: Linearized Axial Stress Results for WRS plus Operating Condition

Weld Residual Stress Analysis for PVNGS3 RV BMI Nozzle Repair (Non-Proprietary)

Figure C-5: Linearized Axial Stress Results for WRS plus Operating Condition

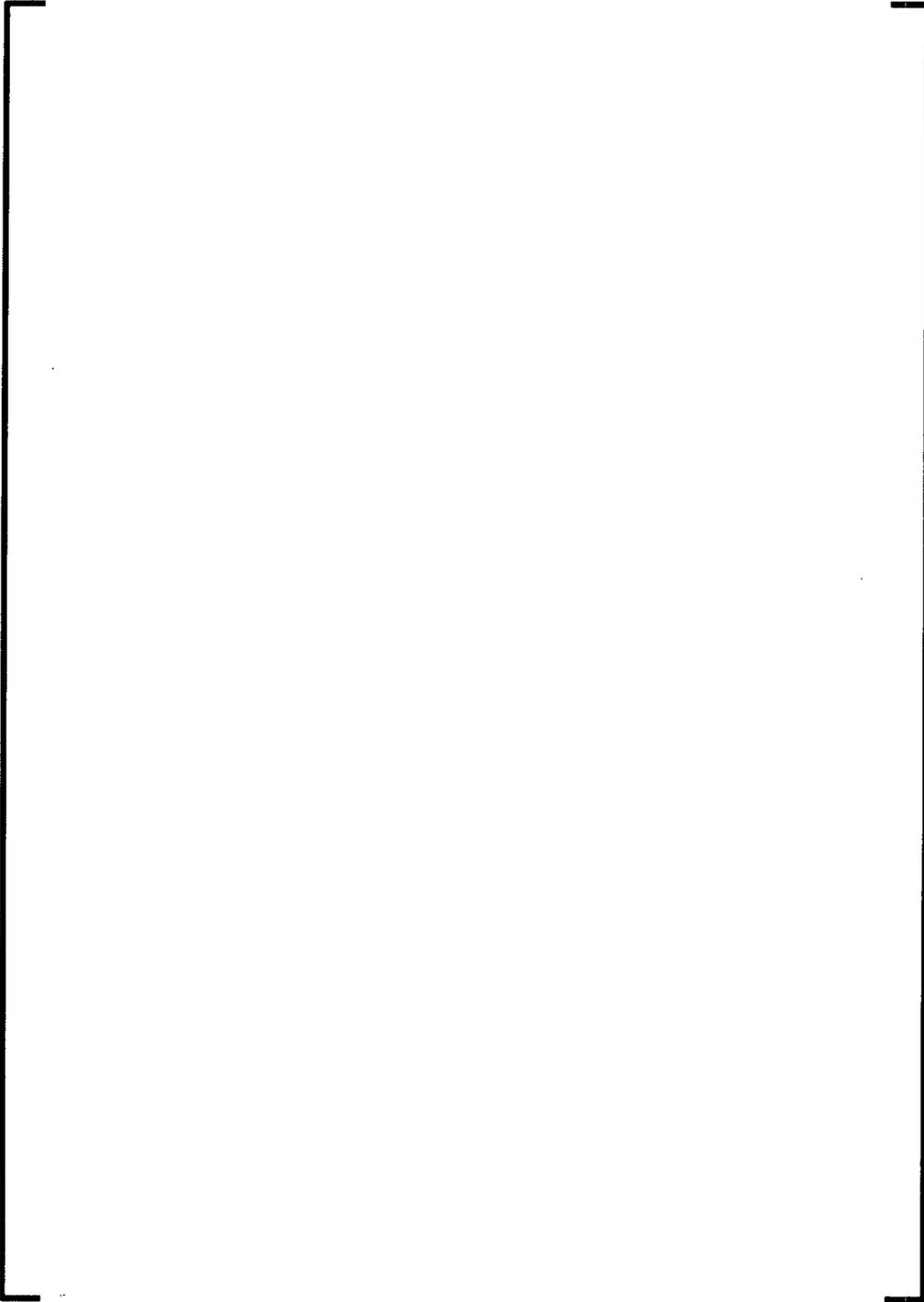Weld Residual Stress Analysis for PVNGS3 RV BMI Nozzle Repair (Non-Proprietary)

Figure C-6: Residual Hoop Stress (psi) for WRS plus Operating Condition

Weld Residual Stress Analysis for PVNGS3 RV BMI Nozzle Repair (Non-Proprietary)
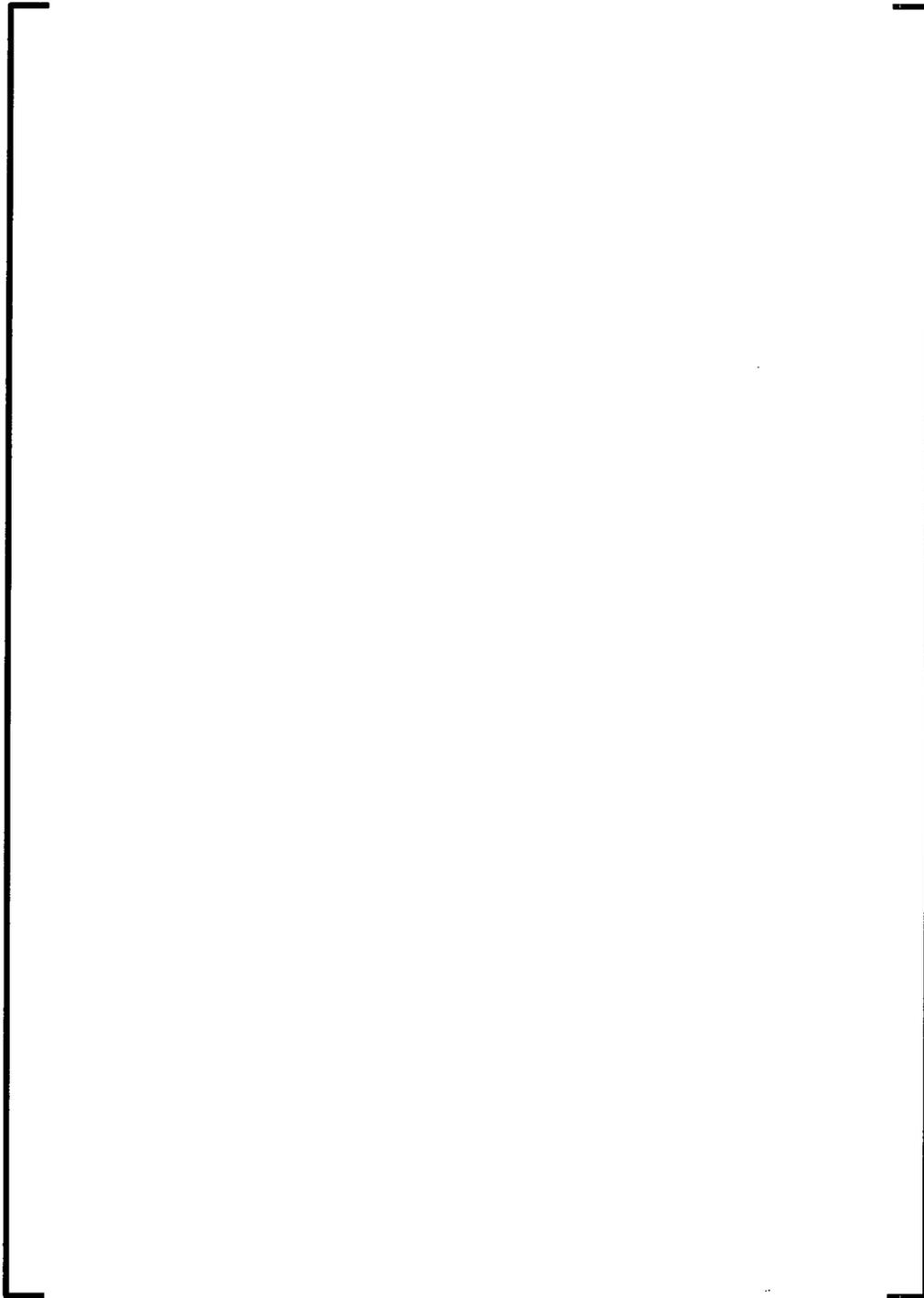
Figure C-7: Residual Axial Stress (psi) for WRS plus Operating Condition